Springer

Acta Mechanica Sinica

CrossMark click for updates

• INVITED REVIEW •

Acta Mech. Sin., Vol. 38, 722323 (2022)
https://doi.org/10.1007/s10409-022-22323-x

A review on gyrotactic swimmers in turbulent flows

Jingran Qiu[1], Cristian Marchioli[2*], and Lihao Zhao[1*]

[1] *Key Laboratory of Applied Mechanics, Department of Engineering Mechanics, Tsinghua University, Beijing 100084, China;*
[2] *Department of Engineering and Architecture, University of Udine, Udine 33100, Italy*

Received October 16, 2022; accepted October 19, 2022; published online November 7, 2022

Many marine plankton species are motile and perform daily vertical migrations, traveling across water columns over distances of tens of meters. It is intriguing that these tiny and slow swimmers can travel in a certain direction within a turbulent environment. One way to do that is by exploiting gravitaxis, which is a form of taxis characterised by the directional movement of an organism in response to gravity. Many plankton species are able to generate a gravitational torque (e.g., due to a non-uniform mass distribution) that reorients them upwards. However, the swimming direction is disturbed by the shearing motions and the velocity fluctuations that characterise oceanic turbulence: these can generate a viscous torque that may destabilize the swimmer. The directed locomotion resulting from the combination of gravitational and viscous torques in a flow is termed gyrotaxis, which is known to lead to a non-uniform spatial accumulation of swimmers in patches or layers. These phenomena depend strongly on the non-linear dynamics that originate from the fluid motions, and the study of gyrotactic swimmers in complex flows is attracting growing attention. Numerical simulations of the Navier-Stokes equations coupled with suitable models of gyrotactic swimmers have proven their capability to provide valuable insight into the dynamical and statistical properties of self-propelled organisms. In this paper, we review recent studies and key findings on gyrotactic swimmers in turbulent flows. First, we introduce the most recent results concerning the orientation and vertical migration of gyrotactic swimmers in isotropic turbulence. Second, we discuss the findings on the accumulation of the swimmers. Last, we review recent progresses concerning the behaviour of gyrotactic swimmers in free-surface turbulence.

Gyrotaxis, Plankton, Turbulence

Citation: J. Qiu, C. Marchioli, and L. Zhao, A review on gyrotactic swimmers in turbulent flows, Acta Mech. Sin. **38**, 722323 (2022), https://doi.org/10.1007/s10409-022-22323-x

1. Introduction

One important source of complexity associated with the modelling and the simulation of phytoplankton interaction with turbulence in water bodies is the motility of the plankton cells. Many phytoplankton species are self-propelled and, even if their swimming speeds are typically smaller than ambient flow speeds, there is well-documented evidence that the interplay between motility and turbulence can result in complex and ecologically important phenomena [1-3]. For instance, some phytoplankton species (e.g., raphidophytes and dinoflagellates) have developed the ability to migrate upward toward the water surface during the day to activate photosynthesis, and downward at night, toward the deeper layers rich in nutrients [4]. It is now well-known that vertical migration is favoured when swimmers can modify the swimming direction by responding to different physicochemical biases, e.g., chemotaxis, gyrotaxis and phototaxis [1]. In this review, we are interested in gyrotaxis, which is perhaps the most widely-studied type of motile response. In particular, we focus on the gyrotactic effect that originates from the competition between a stabilising gravitational torque, which can be produced by a non-uniform mass distribution of the swimmer and favours its orientation along the direction of gravity (gravitaxis), and a destabilising viscous torque, produced by the local shear acting on the swimmer [5,6]. A schematic of a gyrotactic

*Corresponding authors. E-mail addresses: marchioli@uniud.it (Cristian Marchioli); zhaolihao@tsinghua.edu.cn (Lihao Zhao)
Executive Editor: Mingjiu Ni

swimmer is provided in Fig. 1, where the gravitational torque and the viscous torque are visualized together with the displacement between the center of gravity and the center of rotation determined by the non-uniform mass distribution within the cell. Because of gyrotaxis, motile micro-organisms are able to deviate from the streamlines of the underlying flow even if their inertia is small, when not negligible. This capability allows for the formation of densely-populated patches and/or clusters. For instance, plankton can form layers of thickness ranging from centimeters to meters, which last for hours as observed in field experiments [7], this phenomenon being the result of the interaction between gyrotaxis and turbulent shear [8]. Indeed, the rising of gyrotactic micro-swimmers in a turbulent flow represents a nice example of two-phase problem, in which preferential concentration phenomena occur even in the absence of inertia of the dispersed phase. This is just one of the reasons why a great deal of experimental and numerical studies (see Refs. [2,9-17] among others) have been devoted to understanding the role that gyrotaxis.

Experimental studies of gyrotactic swimmers dated back to the famous experiment of Kessler's [18-20], who observed that bottom-heavy plankton in a vertical tube accumulate in different regions when the flow in the tube goes either up or down. Cells accumulate in the center of the tube in a downward flow because the flow shear tilts the orientation of gyrotactic cells towards the center of tube. In an upward flow, the shear is in the opposite direction, so cells accumulate at the wall. Using a horizontal shear flow, Durham et al. [21] observed that gyrotactic plankton is trapped in the regions with high shear, which explains the formation of plankton layers observed in nature [7]. Durham et al. [8] observed that gyrotactic swimmers tend to accumulate in downwelling regions in a simple vertical flow, while De Lillo et al. [9] found that fluid acceleration changes the preferred orientation of gyrotactic swimmers,

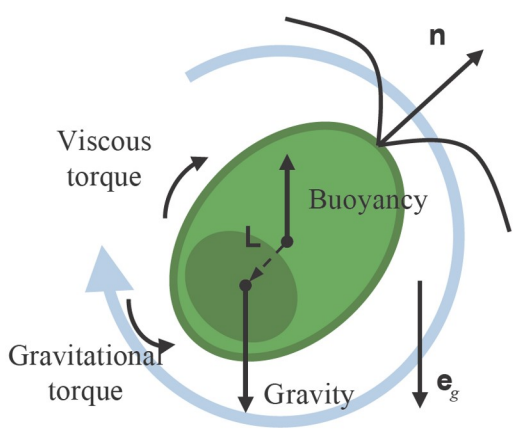

Figure 1 Schematic of a swimmer under the action of viscous and gravitational torques. The light blue arrow indicates the rotation of the carrier fluid.

allowing them to accumulate in strong vortices. In spite of these findings, however, experiments on gyrotactic swimmers are still limited by the difficulty of tracking tiny and massive plankton cells as well as measuring the flow field. This is particularly hard in complex (e.g., inhomogeneous anisotropic) flows or when field measurements have to be performed.

Numerical methods have the advantage that they produce trackable data for both the swimmers and the carrier fluid. Thanks to the growing computational resources, direct numerical simulations may now provide more accurate and comprehensive results, which can be compared directly to experiments [8,21] as well as theoretical results [10,22]. Thanks to this, our knowledge about gyrotactic swimmers has significantly advanced over the last two decades, providing for instance ample evidence that motile particles in homogeneous isotropic turbulence (HIT) accumulate inside the vortices and in downwelling regions [8,10,22], while light and heavy non-motile particles accumulate inside and outside the vortices, respectively [23].

In spite of the wealth of studies available in archival literature, there are very few review articles in which recent findings are summarized and put into perspective. To the best of our knowledge, the most recent review was published by Cencini et al. [15] on how gyrotaxis can produce inhomogeneous phytoplankton distributions, yet considering both laminar and turbulent flows, and focusing on gyrotactic trapping in nonlinear shear flows and in fractal clustering in turbulent flows to demonstrate the usefulness of ideas and tools borrowed from dynamical systems theory. In this review, we try to complement the survey of Ref. [15] by also concentrating on gyrotaxis as paradigmatic model for phytoplankton motility in flows, but we consider a wider variety of turbulent flows (going beyond HIT) and we examine the effect of gyrotaxis not only on preferential concentration but also on the orientation and vertical migration of the swimmers, looking at the impact produced by processes such as stratification [11], shearing generated by winds [13], interaction of the swimmers with a free surface mimicking the air-water interface [12].

2. Model of gyrotactic micro-swimmers

Gyrotactic swimmers are usually modeled as spherical or ellipsoidal particles with motility [8-13,21]. According to the typical parameters of plankton (Table 1), one estimates the length and swimming velocity to be of the order of 10^{-4} m and 10^{-3} m/s, respectively. Thus, the particle Reynolds number is estimated as $Re_p = \mathbf{v}_s L / \nu \approx 0.1$, under which case the effect of finite particle size is negligible and a point-particle model is justified. The Stokes number,

$St = \tau_p / \tau_f$, quantifies the inertia of particle, where τ_p and τ_f are the response time of particle and the characteristic time scale of fluid flow, respectively. The Stokes number is usually negligibly small for plankton, which indicates that the particle inertia can be neglected, i.e., the force and torque on a plankton are negligibly small. Therefore, the following inertia-less model has been widely used in earlier studies:

$$\dot{\mathbf{x}} = \mathbf{v}, \tag{1}$$

$$\mathbf{v} = \mathbf{u} + \mathbf{v}_s + \mathbf{v}_g, \tag{2}$$

$$\dot{\mathbf{n}} = \boldsymbol{\omega} \times \mathbf{n}, \tag{3}$$

$$\boldsymbol{\omega} = \boldsymbol{\Omega} + \Lambda \mathbf{n} \times (\mathbf{S} \cdot \mathbf{n}) - \frac{1}{2B} \mathbf{n} \times \mathbf{e}_g \tag{4}$$

Here, $\dot{\mathbf{x}}$ and $\mathbf{n}$ are the position and orientation vector (e.g., the direction of symmetry axis) of a swimmer, $\mathbf{v}$ and $\boldsymbol{\omega}$ are the velocity and angular velocity of a swimmer, respectively. The three terms on the right-hand-side (r.h.s.) of Eq. (2) denote the contributions of fluid velocity at the particle location $\mathbf{u}$, the swimming velocity $\mathbf{v}_s$, and the settling velocity $\mathbf{v}_g$. A swimmer is assumed to swim with a certain speed in the direction of its orientation, giving as $\mathbf{v}_s = v_s \mathbf{n}$. In nature, swimmers are usually slightly heavier than water (see Table 1) so they are subject to a settling velocity. In the limit of $St << 1$, the settling velocity is given by the Stokesian settling velocity [24-26] $\mathbf{v}_g = v_g^{\perp} \mathbf{e}_g + \left(v_g^{\parallel} - v_g^{\perp}\right)(\mathbf{e}_g \cdot \mathbf{n})\mathbf{n}$, where $v_g^{\parallel}$ and $v_g^{\perp}$ are the terminal velocities attained when a swimmer aligns with and perpendicular to the gravity direction, respectively, and $\mathbf{e}_g$ is the unit vector in the direction of gravity.

The orientation of a swimmer is subjected to the fluid velocity gradients and the gyrotaxis torque. The first two terms in Eq. (4) denote the contribution of fluid vorticity $\boldsymbol{\Omega}$ and strain rate $\mathbf{S}$, where $\Lambda = (\lambda^2 - 1)/(\lambda^2 + 1)$ is the shape factor, with λ being the aspect ratio of an ellipsoid. The third term denotes the contribution of the gyrotactic torque [19], where the reorientation timescale, B, is the timescale that a swimmer takes to retain the stable orientation under the gyrotactic torque [27]. The time scale B can be calculated by the balance of the torques acting on a swimmer. For example, a particle of mass m in a quiescent fluid with viscosity ν and density ρ_f, is subjected to the torque due to viscous fluid, $\mathbf{T}_J = -6\pi a \rho_f \nu \mathbf{C} \cdot \boldsymbol{\omega}$, and to the gyrotactic torque $\mathbf{T}_g = m\mathbf{L} \times g$. Here, a is the length of semi-minor axis of an ellipsoid, $\mathbf{L}$ is the offset vector between the center of mass and the center of buoyancy, and $\mathbf{C}$ is the resistance coefficient of an ellipsoid, respectively. Because we neglect the total torque on a particle, $\mathbf{T}_J$ is balanced with $\mathbf{T}_g$. For simplicity, we assume $\mathbf{L}$ to be opposite to $\mathbf{n}$ for a bottom-heavy swimmer. Using Eq. (4), we obtain the expression $B = 3\pi a \rho_f C_{\perp} / mgl$ [27], where $C_{\perp}$ is the resistance coefficient of an ellipsoidal particle rotating with its minor axis [26].

Many previous studies [8,10-13,19,21] have shown that a stable orientation is attained upon alignment with or against the direction of gravity, because gravity usually provides the major contribution of acceleration that reorients the swimmer. However, in certain circumstances, the fluid acceleration is comparable to gravity. This changes the preferential orientation under gyrotaxis, and causes a different kind of clustering effect which leads to swimmers' accumulation in high vorticity regions [9]. Recently, the fluid inertial effect on swimmers has been considered [28-30]. Qiu et al. [29] showed that the effect of the fluid inertial torque can be quantified by an effective reorientation timescale, and that the swimmers exhibit a strong preferential alignment in the upward direction when the timescale is of the same order of the Kolmogorov timescale. This suggests that the fluid inertial torque may provide a different mechanism of gyrotaxis, by which the upward orientation of the swimmers can be stabilized.

The behaviour of gyrotactic swimmers is governed by two dimensionless numbers. The reorientation timescale is described by $\Psi = B / t_f$ (also referred to as stability number), and the swimming velocity is described by $\Phi = v_s / u_f$ (also referred to as swimming number), where t_f and u_f are the typical time and velocity scales of the fluid flow, respectively. For HIT, t_f and u_f can be chosen as the Kolmogorov scales of the flow [8,10,22]. However, the typical scales of complex flows, characterized by inhomogeneity and anisotropy for instance, may vary in space and time. For example, in a wall-bounded turbulent flow, the turbulence is more intensive near the wall due to shear. The time and velocity scales near the wall are shorter and larger, respectively, compared with the regions far away from the wall. The behaviour of gyrotactic swimmers is, therefore, expected to be different because the two dimensionless numbers, Ψ and Φ, change locally due to the varying scales of flow.

3. Orientation and vertical migration

The most striking macroscopic effect of gyrotaxis is its in-

Table 1 Typical parameters of plankton in the ocean

Parameters	Values
Length (μm) [31-33]	20-300
Swimming speed (μm/s) [31-33]	100-1000
Reorientation time (s) [4,18,21,34]	0.2-30
Aspect ratio [35]	1-8
Density (g/cm^3) [33]	1.06-1.09

fluence on the orientation of a swimmer. Understanding the orientation of gyrotactic swimmers is important because it allows for the prediction of the direction and efficiency of vertical plankton migration. According to Eq. (4), the rotation of a swimmer is determined by the effect of gyrotactic and the effect of fluid vorticity and strain rate along the Lagrangian trajectory of a swimmer. Because the gyrotactic term has a magnitude not larger than $(2B)^{-1}$, the swimmer will tumble when the importance of the vorticity and strain rate terms is sufficiently large. Otherwise, the swimmer is expected to attain an equilibrium orientation if the effect of fluid velocity gradients is small compared with that of gyrotaxis. This can be seen from the simplest case, in which the swimmer is spherical and moves in a steady and uniform shear flow. This allows for a constant vorticity along the trajectory of a swimmer and a vanished strain rate term in Eq. (4). In a special case that the vorticity is perpendicular to the preferred orientation of gyrotaxis indicated by $\mathbf{e}_a$, Eq. (4) can be substantially simplified as

$$\dot{\theta} = \omega - \frac{1}{2B}\sin\theta, \tag{5}$$

where θ is the angle between the swimming direction and the preferred orientation under gyrotaxis, i.e., $\cos\theta = \mathbf{n}\cdot\mathbf{e}_g$. When $2\omega B \leq 1$, the equilibrium orientation obeys $\sin\theta = \omega B$, which gives two equilibrium orientations, but only the one with $\theta < \pi/2$ is stable. When $2\omega B > 1$, the swimmer tumbles and there is no equilibrium orientation. In a general case, however, the rotational dynamics given by Eq. (4) cannot be simplified as Eq. (5) because the vorticity is not always perpendicular to $\mathbf{e}_g$. In the latter case, the dynamics again have equilibrium points for $2\omega B > 1$, leading to a swirling swimming trajectory around the direction of vorticity, as shown in Fig. 2. This is well documented by the analysis performed by Pedley and Kessler [27], Thorn and Bearon [36].

In nature, plankton usually resides in a turbulent environment, experiencing a fluctuating fluid flow along their trajectories. In general, the orientation of gyrotactic swimmers depends on two timescales which correspond to the effect of gyrotaxis and fluid velocity gradients, and they are denoted by B and t_η, respectively. The relation between these time scales determines the behaviour of gyrotactic swimmers in turbulence. An important limit is when turbulence is weak, which corresponds to $B << t_\eta$ and thus to $\Psi << 1$. In this limit, the effect of turbulence can be regarded as a perturbation from the stable orientation $\mathbf{n} \approx -\mathbf{e}_a$. In such a case, a spherical swimmer has equilibrium orientation $\mathbf{n} \approx \left(\Psi\omega_y / t_\eta, -\Psi\omega_x / t_\eta, 1\right)$ assuming $\mathbf{e}_g = (0, 0, -1)$ [8,37]. This is useful for analysing patchiness, as discussed in the next section.

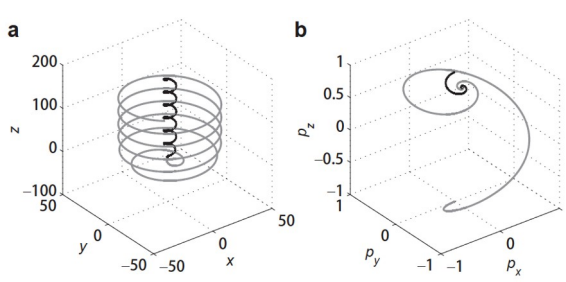

Figure 2 Typical trajectories of gyrotactic swimmers with $2\omega B > 1$. **a** Position and **b** orientation. The vorticity is in z-direction, and $\mathbf{e}_a = (\sin(\pi/4), 0, \cos(\pi/4))$. The notation p in **b** stands for the swimming direction, which is denoted by **n** in this paper (Figure taken from Ref. [36]).

When turbulence is intense, swimmers have no deterministic orientation. In this case, it is more useful to discuss the probability distribution of the orientation of a population of swimmers. Lewis [38] suggested that the orientation of gyrotactic swimmers in a turbulent flow satisfies a Fokker-Planck equation, which is similar to the rotatory Brownian motion [39,40]. The only difference is that for Brownian motion the rotational diffusivity originates from the molecular thermal motion, while for turbulence an effective diffusivity is caused by the random fluctuation of velocity gradients. Lewis [38] obtained the steady distribution of orientation for spherical gyrotactic swimmers in an isotropic turbulence as follows:

$$G(\theta) = \frac{\beta e^{\beta\cos\theta}}{2\sinh\beta}, \tag{6}$$

$$\beta = \frac{B^{-1}}{2D_{\text{eff}}}, \tag{7}$$

where G is the probability distribution of orientation θ, and D_{eff} is the effective diffusivity. The distribution given by Eq. (6) describes well the orientation of gyrotatic swimmers in random flows [38] as shown in Fig. 3, but D_{eff} is treated as an open parameter in the model. To understand the underlying physics, Fouxon and Leshansky [37] derived the Fokker-Planck equation from the dynamics of Eqs. (1)-(4), and obtained the same distribution of Eq. (6) in the limit of turbulence being described as Gaussian noise. In other words, the correlation time of the turbulent velocity gradients experienced along the trajectory of a swimmer needs to be much less than the timescale of the change in orientation. This requires either $\Psi >> 1$ or $\{\Psi < 1, \Phi\Psi >> 1\}$. The first condition corresponds to extremely weak gyrotaxis, while the second corresponds to the swimmers moving through the smallest flow scale in a short time so that the velocity gradients decorrelate quickly.

The analyses just discussed are mainly for spherical swimmers. The theoretical analysis with non-spherical swimmers is expected to be more difficult, since they are subjected to a non-zero strain rate term, appearing in Eq. (4), which depends on the instantaneous orientation. A direct result is that elongated swimmers in turbulence show a

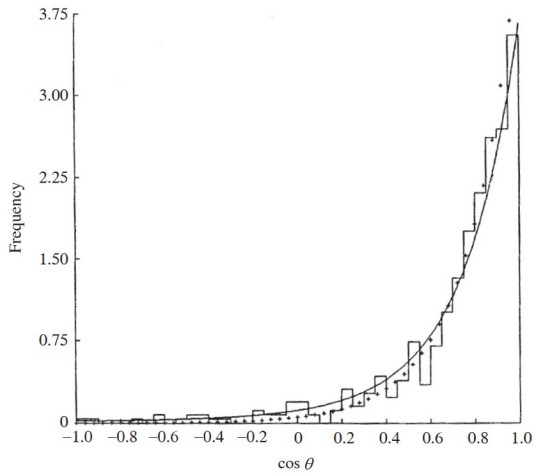

Figure 3 Probability distribution function of the orientation of swimmers in a random flow, taken from Ref. [38]. The histogram represents the distribution obtained by numerical simulation of swimmers in the random flow. The crosses represent the distribution predicted by Eq. (6). The solid line represents the theoretical prediction proposed by Ref. [38]. B^{-1} = 1.6931, D_{eff} = 0.17.

preferential orientation with respect to the first and second eigenvectors of local strain rate tensor [14], which is similar to non-motile elongated tracers [41,42]. This preferential alignment with local fluid structures leads to a longer timescale for an elongated swimmer to align with the preferred direction of gyrotaxis $-\mathbf{e}_g$, which weakens the alignment in $-\mathbf{e}_g$ [14]. Recently, Borgnino et al. [43] have examined the orientation statistics of spheroidal, axisymmetric microswimmers, with the shapes ranging from disks to rods, in chaotic turbulence-resembling flow. They showed that alignment is caused by the combined effect of (1) the correlations of fluid velocity and its gradients along the path followed by the swimmer and (2) the fore-aft symmetry breaking due to both swimming and non-sphericity of particle shape. Such alignment was found to be independent of the underlying flow evolution, but its role for gyrotactic swimmers needs to be further investigated.

4. Patchiness and preferential sampling

Patchiness of swimming plankton plays a crucial but complex role in the life of these organisms. Forming patchiness increases the rate of mating, which benefits their reproduction. However, patchiness can also be harmful because it increases the grazing of predators [44] as well as the competition in nutrients between neighbouring individuals [45]. Understanding the patchiness of swimmers in turbulence is important because it provides mechanical interpretation of the different swimming behaviour among species that may result in different levels of patchiness.

Gyrotactic swimmers are known to form patches. Kessler [18] observed the accumulation of swimming plankton in the center of a downward pipe flow. Plankton also forms thin layers when they encounter strong flow shear [21]. De Lillo et al. [9] observed that swimming plankton accumulates in the core of strong vortices because centrifugal acceleration aligns the swimming direction to the center of the vortices, while dead cells remain randomly distributed. Gyrotactic swimmers in turbulence also form patchiness as reported by numerical studies based on direct numerical simulations [8,9,14,22,46]. This is nontrivial because turbulence often acts as a mixing process. For instance, passive tracers are advected and dispersed randomly in a turbulent flow because they passively follow the fluid streamlines. On the contrary, swimmers can move across the streamlines and form patches if the swimming direction is preferential due to the gravity or shape effects, as discussed below. Interestingly, simulations in HIT show that swimmers tend to accumulate inside the vortices or in downwelling regions when clustering is dictated by the vertical stability (high stability number) [8,10,22], but accumulate outside the vortices when clustering is dictated by the swimming velocity (high swimming number) [47].

To analyse the patchiness on the population level of swimmers, we need to quantify the degree of patchiness. The fractal dimension of the patches, referred to as D hereinafter, is one of the most commonly used indicators. It can be calculated from the radial distribution function (i.e., the possibility of finding a pair of swimmers at a distance r):

$$g(r) = \frac{\mathrm{d}N_r}{N(N-1)\mathrm{d}r}, \tag{8}$$

$$g(r) \sim r^D, \tag{9}$$

where N is the total number of swimmers counted in the calculation of g, and D is defined as the exponent of $g(r)$ at small r. Obviously, D is equal to the spatial dimension if swimmers are randomly distributed. However, D is smaller than the spatial dimension when swimmers form patches, which is also called fractal clustering. In addition to the fractal dimension, Voronoï tessellation is also commonly used to analyse the patchiness of particles [48,49] or swimmers [17]. Based on the instantaneous swimmer position, the Voronoï tessellation splits the spatial domain into many Voronoï polyhedrons. Each polyhedron represents the spatial region that is closest to the unique swimmer contained in the polyhedron, so the volumes of polyhedrons are smaller when the swimmers form a local cluster. The distribution of the volumes of Voronoï polyhedrons implies rich information about patchiness. The effect of gyrotaxis on patchiness of swimmers was first studied by Durham et al. [8] who showed the relation between D and Φ and Ψ for

spherical swimmers, as shown in Fig. 4a. D is the smallest when $\Psi \sim 1$, and decreases as Φ becomes larger in this regime of Ψ. This means that swimmers form stronger patches if they swim fast compared to the Kolmogorov velocity scale and their gyrotactic torque is comparable to the effect of vorticity. It is believed that patchiness is a result of preferential sampling in downwelling or upwelling regions. This is supported by the observation that the trend of vertical fluid velocity sampled by gyrotactic swimmers, u_z, is similar to the trend of D over Φ and Ψ [8], as shown in Fig. 4b.

The shape of the swimmer also has a significant effect on the patchiness. In the limit of infinite large Ψ, namely no gyrotactic torque, elongated swimmers still form patchiness whereas spherical swimmers do not. Zhan et al. [14] suggested that the patchiness of non-gyrotactic elongated swimmers is due to the turbulent flow topology they sample, because elongated particles are known to align with the direction of local vorticity as well as the first and second eigendirections of strain rate [41,42]. This kind of preferential alignment still exists when elongated particles swim [14]. When a swimmer experiences gyrotactic torque (Ψ is limited), the alignment with respect to the eigendirections of the strain rate leads to different levels of patchiness for spherical and elongated gyrotactic swimmers. As observed by numerical simulations [14,22] and theoretical studies [10], spherical swimmers cluster more than elongated swimmers when Ψ is small, while the opposite happens when Ψ is large, as shown in Fig. 4c. Zhan et al. [14] concluded that elongated swimmers are more likely to be influenced by the shear of flow than spherical ones. As a result, it is more difficult for the elongated swimmers to reach an equilibrium orientation due to gyrotaxis and form patches compared to spherical swimmers with a small Ψ. On the contrary, when Ψ is large, elongated swimmers form a stronger patchiness compared with spherical ones.

One of the most intriguing problems is to build up the dependence of swimmers' patchiness in turbulence on the main dimensionless numbers characterizing the problem, i.e., Φ, Ψ, and Λ for the swimming speed, the gyrotactic torque, and the shape of swimmers, respectively. The dependence is complex because patchiness results from the combined action of turbulence dynamics, swimming and preferential alignment. To the best of our knowledge, yet no universal model is built that can describe patchiness in HIT for any value of Φ, Ψ, and Λ. Nevertheless, efforts have been made in some limits in which the dynamics can be simplified. First of all, for spherical swimmers with $\Psi << 1$, Eq. (3) yields $\mathbf{n} \approx \left(\Psi\omega_y / t_\eta, -\Psi\omega_x / t_\eta, 1\right)$ as discussed in Sect. 3, where the direction of gravity acceleration is assumed to be in the negative direction of z-axis. Replacing $\mathbf{n}$ in the swimming velocity $\mathbf{v}_s = \mathbf{n}v_s$, and taking the divergence of the left- and right-hand-side of Eq. (2), Durham et al. [8] obtained the following relationship:

$$\nabla \cdot \mathbf{v} = -\Psi\Phi\nabla^2 u_z, \tag{10}$$

where $\nabla \cdot \mathbf{u} = 0$ is assumed and the settling velocity has been neglected. The accumulation of swimmers is indicated by the negative divergence of the velocity of swimmers, which means that swimmers accumulate in the regions of large $\nabla^2 u_z$. In HIT, $\nabla^2 u_z$ is negatively correlated with u_z, as can be seen from the energy dissipation of turbulence [8,50]:

$$\varepsilon = \nu\left\langle|\nabla \mathbf{u}|^2\right\rangle = -\nu\left\langle \mathbf{u} \cdot \nabla^2 \mathbf{u}\right\rangle = -3\nu\left\langle u_z \cdot \nabla^2 u_z\right\rangle > 0. \tag{11}$$

Therefore, swimmers with small Ψ preferentially sample downwelling regions, and the intensity of the sampling is proportional to $\Psi\Phi$. Equation (10) also implies that strong gyrotactic swimmers in an incompressible fluid flow can be seen as tracers in a weakly compressible fluid with a divergence given by $-\Psi\Phi\nabla^2 u_z$. In this case, the fractal dimension D is predicted as [8,51,52]

$$D = 3 - a(\Psi\Phi)^2, \tag{12}$$

which is in good agreement with numerical results.

The non-spherical shape of swimmers brings in more

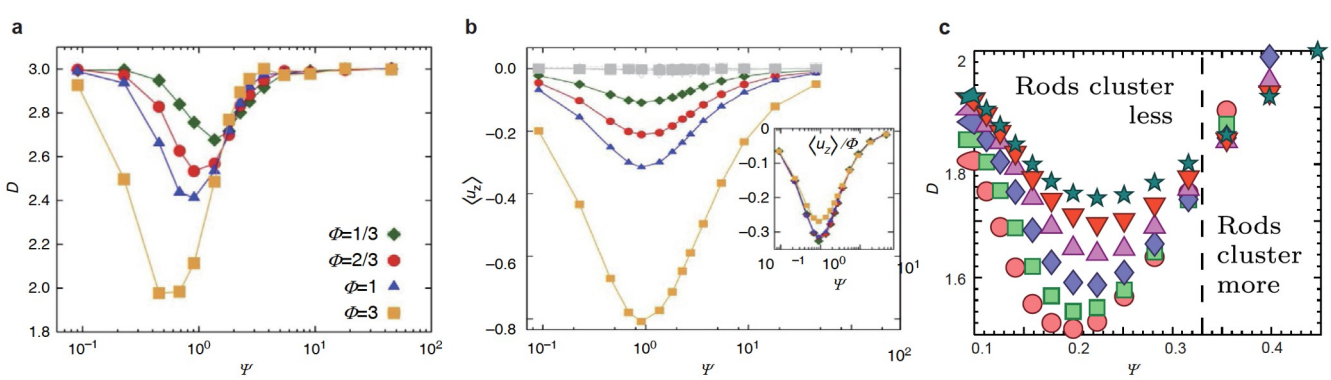

Figure 4 **a** Fractal dimension of spherical swimmers as a function of Ψ and Φ in HIT, taken from Ref. [8]. **b** The vertical fluid velocity sampled by spherical swimmers in HIT, adopted from Ref. [8]. **c** The fractal dimension of swimmers of different aspect ratio in two-dimensional random flow, taken from Ref. [10]. Circles: $\Lambda = 0$; squares: $\Lambda = 0.2$; diamonds: $\Lambda = 0.4$; triangles: $\Lambda = 0.6$; inverted triangles: $\Lambda = 0.8$; stars: $\Lambda = 1.0$.

complexity because of the strain rate term in Eq. (4). Gustavsson et al. [10] studied the preferential sampling of flow regions and patchiness with respect to three dimensionless numbers: Λ, Φ and Ψ. Using statistical model for the fluid phase, these authors gave an analytical prediction of fractal dimension and u_z sampled by swimmers with a large or small Φ in the limit of $Ku << 1$, where Ku is the Kubo number, a dimensionless number that quantifies the time correlation of the flow. The predicted fractal dimension is in good agreement with direct numerical simulations [14] as shown in Fig. 4c. Moreover, Gustavsson et al. [10] suggested that spherical swimmers sample downwelling regions, but elongated swimmers can sample upwelling regions if swimming speed is larger than a critical value. This trend has been also examined by direct numerical simulations of HIT [22]. Figure 5a shows that the critical swimming speed increases as Ψ decreases. Figure 5b shows that the relationship between the critical swimming speeds and Ψ collapses at different Reynolds number as long as the swimming speed is scaled by the root-mean-square fluid velocity $u_{\rm rms}$, $\Phi_{\rm L} = v_s / u_{\rm rms}$. This suggests the preferential sampling effect may be related to the large scale motions of fluid [22].

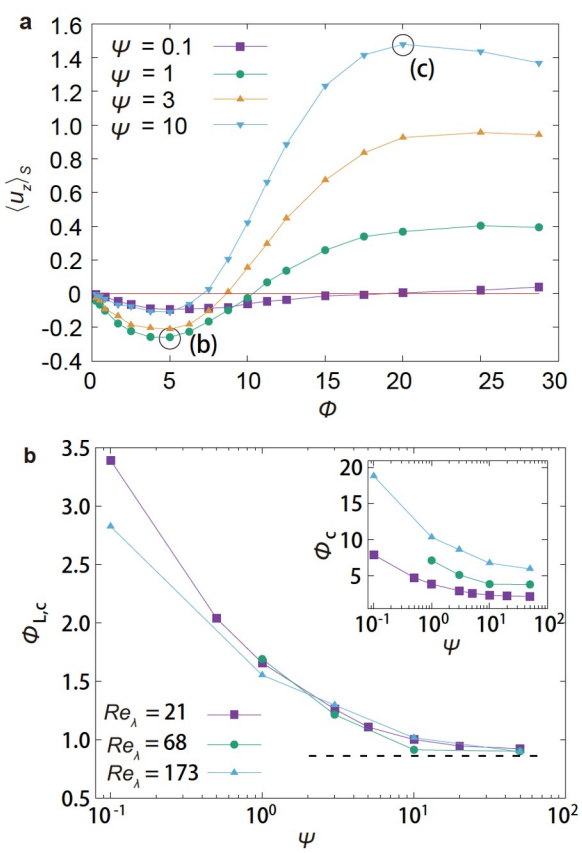

Figure 5 **a** Vertical fluid velocity sampled by elongated swimmers in HIT. **b** The critical value of $\Phi_{\rm L}$ and Φ (inset) for swimmers with different Ψ to sample upwelling regions. Both figures are taken from Ref. [22].

5. Gyrotactic swimmers in free-surface turbulence

The behaviour of the swimmers is significantly affected by the properties of the turbulent flow they evolve in. In particular, compared with the case of isotropic turbulence, motility leads to a different gyrotaxis when coupled with shear in the form of vertical gradients in horizontal fluid velocity, which are typical of air-water interfaces. In an effort to advance current understanding of how gyrotactic swimmers propel themselves near and below an air-water interface, several studies [11-13] have recently investigated swimmer dynamics for the reference case of turbulent open channel flow bounded by a free-surface at the top and a solid wall at the bottom. This setup mimics the dynamics of phytoplankton in water bodies when surface waves and ripples are smooth or absent, also reproducing the main features of a fluctuating heterogeneous environment characterised by a marked separation between the forcing scale and the dissipation scale [12]. Figure 6 provides a visual rendering of the spatial distribution that can be attained by gyrotactic swimmers at the free surface, showing that swimmers tend to sample the upwelling and downwelling regions on the surface [12]. These regions can be identified by means of the surface divergence [42], defined as

$$\nabla_{\rm 2D} = \frac{\partial u_x}{\partial x} + \frac{\partial u_y}{\partial y} = -\frac{\partial u_z}{\partial z}, \tag{13}$$

where u_x and u_y are the (streamwise and spanwise) fluid velocity components parallel to the free-surface, whereas u_z is the fluid velocity component normal to the surface. Fluid upwellings generate regions of local flow expansion ($\nabla_{\rm 2D} > 0$) while fluid downwellings generate regions of local compression ($\nabla_{\rm 2D} < 0$). The most evident feature of swimmer spatial distribution is the formation of highly-concentrated clusters that originate from the interaction between individual cells and surface flow structures. Such macroscopic manifestation in free-surface turbulence is also common to floaters and motile particle [3,13,53,54]. Because of gyrotaxis, swimmers cannot leave the surface following flow motions: they can only leave velocity sources (red areas in Fig. 6) and collect into velocity sinks (blue areas in Fig. 6), organizing into clusters that are advected passively by the mean flow until a subsequent burst hits the cluster causing its reshaping. Eventually sharp filamentary patches characterised by high concentration of swimmers are produced, which correlate very well with the rapidly-changing patches of $\nabla_{\rm 2D}$ [3]. The presence of localized filamentary regions where swimmers tend to accumulate under the action of the local flow appears to be a rather robust feature of swimmer dynamics in turbulence even if the Reynolds number dependence does not seem to be universal [55].

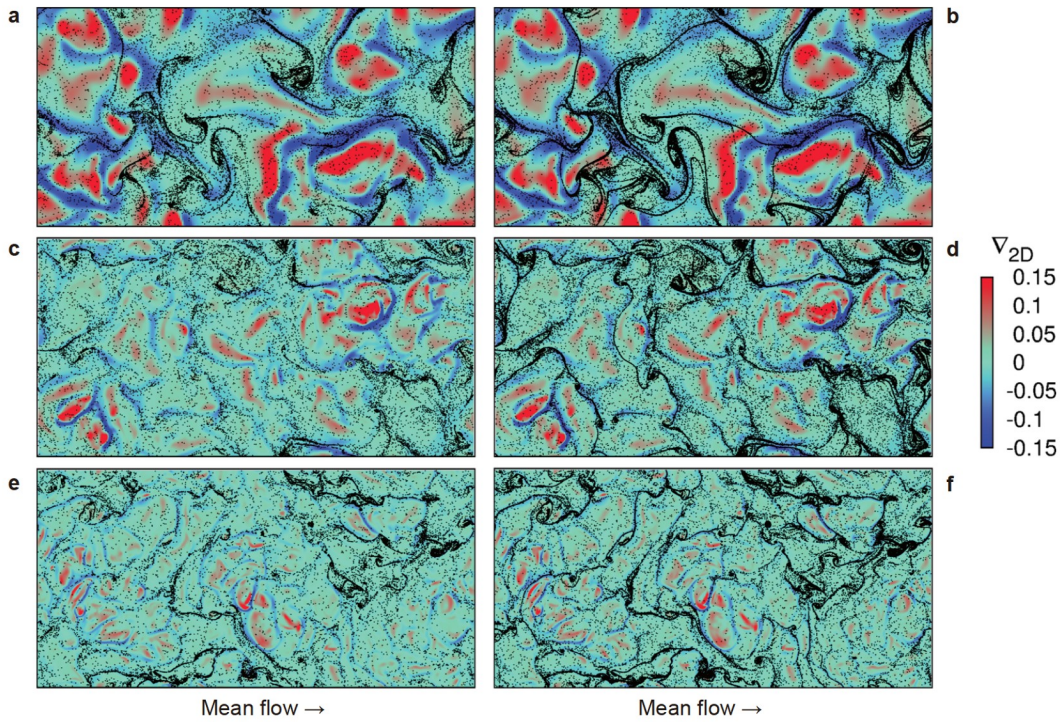

Figure 6 Instantaneous spatial distribution of gyrotactic micro-swimmers on the free surface of a turbulent open channel flow at varying flow shear Reynolds number and stability number. **a**, **b** $Re_\tau = 170$; **c**, **d** $Re_\tau = 510$; **e**, **f** $Re_\tau = 1020$. Left-hand panels refer to low-gyrotaxis swimmers (low stability number), right-hand panels refer to high-gyrotaxis swimmers (high stability number). Figure taken from Ref. [12].

The surface distribution shown in Fig. 6 is clearly produced by the surfacing of the swimmers, which depends on the ability of the swimmers to exploit the large-scale advective motions that characterise the turbulence below the surface, as shown in Ref. [12]. Such ability depends on the vertical stability of the swimmers, what matters being the ratio between their characteristic re-orientation time and the Kolmogorov time scale, τ_K (which is the characteristic time scale of the small turbulent structures in the flow). As shown in Ref. [12], large-scale advection dominates vertical motion when the stability number, scaled on the local Kolmogorov time scale of the flow, is larger than unity. When this condition is met, migration towards the surface is enhanced, particularly at low Reynolds number since swimmers can rise exploiting the surface renewal motions that originate from the bottom-boundary turbulent bursts.

Migration is hindered when the stability number, scaled on the local Kolmogorov time scale of the flow, is below unity. When this condition is met, small-scale effects become more important, particularly at high Reynolds number, since the bottom-boundary bursts are less effective in bringing fluid to the surface. Therefore, a Kolmogorov-based stability number can be defined as

$$\Psi_K^+ = \frac{1}{2B}\tau_K = \Psi^+\tau_K^+, \tag{14}$$

where the superscript + represents dimensionless variables in wall units and $\Psi^+ = \nu/\left(Bu_\tau^2\right)$. Note that the definition of Ψ^+ differs from the definition of Ψ used in the previous section. A larger Ψ^+ means a stronger stability whereas larger Ψ stands for a weaker stability. This definition discriminates the different roles played by the small and large scales of the flow in determining the ability of vertical migration of swimmers, and it establishes a threshold (namely $\Psi_K^+ \cong 1$ when τ_K^+ is equal to the maximum value within the flow, which is attained at the free-surface) beyond which the capability to reach the free surface and form clusters saturates [12]. This is confirmed quantitatively in Fig. 7, where the values of the swimmer concentration at the free surface, C/C_0, and the corresponding values of Ψ_K^+ are shown for the different values of the flow shear Reynolds number Re_τ and of the stability number Ψ^+, at self-propelling speeds that are typical of the most common phytoplankton species. Whenever $\Psi_K^+ < 1$, namely whenever the time scale of gyrotaxis is large compared with that of small flow structures, swimmers cannot overcome the destabilizing influence of these small-scale structures on vertical migration and their ability to reach the surface through the large-scale advective structures of the flow is reduced. This leads to a reduced accumulation at the free-surface. The opposite occurs when $\Psi_K^+ >$ 1, namely when the time scale of gyrotaxis is small com-

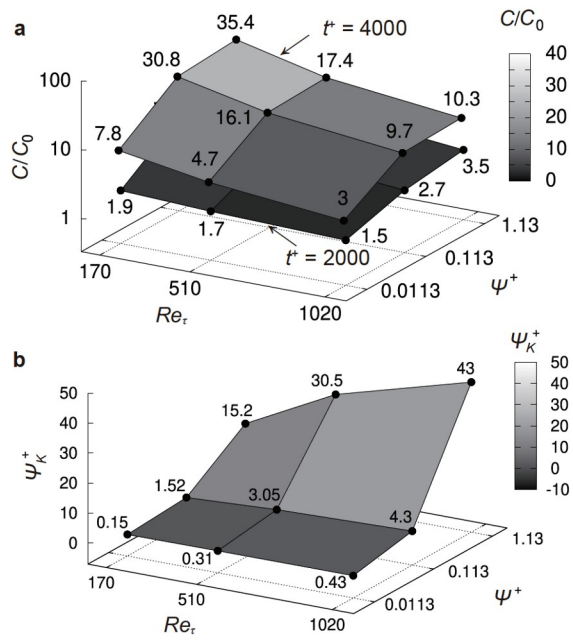

Figure 7 Swimmer concentration **a** and corresponding Kolmogorov-based stability number **b** on the free-surface at varying shear Reynolds number and stability number. Here, $\psi^+ = 0.0113$, $\psi^+ = 0.113$, $\psi^+ = 1.13$ represent swimmers with low, intermediate and high gyrotaxis, respectively. Figure reproduced with data from Ref. [12].

pared with that of the small flow structures: swimmers respond quickly to gravity and this gives them the ability to counteract small-scale destabilizations and exploit large-scale advection to reach the surface, thus enhancing accumulation. The role of the small turbulent scales was also recognized by Jaccod et al. [55], who focused on their impact on the statistics of plankton density fields at very fine scales in a flow past an idealized island. Understanding the interaction between swimmers and flow scales is important because swimmers can only sense and react to the local flow information while having no access to the global information: therefore, the swimming direction can be adapted solely based on the local flow vorticity [56].

The overall surfacing and clustering behaviour of the gyrotactic swimmers can be influenced by a number of factors related to the specific features of the flow. For instance, the acceleration of the fluid surrounding the swimmers can modulate their ability to rise in upwellings and sink in downwellings, especially in high-Re_τ flows, as a consequence of a stronger tendency of the swimmers to sample high-vorticity regions of the flow [9,15]. In Ref. [47], highly-clustered swimmers were found to be associated to an increase in the acceleration frequency distribution, suggesting a direct influence of acceleration on clustering.

Also, the occurrence of regions of strong local shear has been shown to affect surfacing, as in the case of a wind-sheared flow. Indeed, wind-induced shear has a profound effect on the transport and mixing processes in the upper layers of large water bodies, particularly in the oceans where it controls the vertical distribution and residence time of phytoplankton species rising and sinking across the near-surface region [57,58].

The interplay between wind-induced shear and gyrotaxis in a three-dimensional turbulent flow was studied by Ref. [13], with the aim of assessing the conditions under which the trapping phenomena previously described for a simple free-shear surface can still take place. In these studies, the choice of considering a wind-sheared turbulent flow with a flat undeformable surface was made. This choice is based on the findings of several previous studies [3,54,59,60], which have shown that light particles moving at the deformed free surface of a turbulent flow are subject to clustering mechanisms that come from the horizontal divergence in the surface: These mechanisms induce a compressible effect similar to the one observed for flat surface. In addition, transfer mechanisms across a gas-liquid interface like the one considered in Ref. [13] are controlled mainly by coherent structures on the liquid side for wind-driven turbulence under the condition of low wind velocity (and no wave breaking).

Figure 8 provides a qualitative picture of these phenomena for three different flow configurations, produced by applying a suitable constant-stress boundary condition at the top surface of the flow domain to model the wind-induced forcing: free-slip surface without wind; co-current wind blowing in the streamwise flow direction; counter-current wind blowing against the streamwise flow direction. Figure 8 shows that the flow topology (velocity sources/sinks) and the morphology of the surface clusters formed by the swimmers depend not only on gyrotaxis but also on the wind forcing. In the co-current wind case (middle-row panels in Fig. 8), a sharper alternation of velocity sources and sinks with smaller spatial extent is observed and only swimmers with high gyrotaxis can cluster. In the counter-current wind case (bottom-row panels in Fig. 8), surface flow structures more rarely appear in the form of strong sources/sinks and swimmers are able to cluster already at intermediate gyrotaxis.

These observations can be correlated with the orientational behavior of the swimmers, which is shown in Fig. 9 with reference to the vertical direction only. Note that $\langle p_z \rangle = 1$ indicates swimmers aligned with the vertical direction, whereas $\langle p_z \rangle = 0$ indicates swimmers moving in the horizontal plane. The most interesting wind-related effects are obtained for the swimmers with intermediate gyrotaxis, since those with low gyrotaxis are always destabilized by the local turbulent fluctuations while those with high gyrotaxis are always stabilized by gravitaxis. Compared with the free-slip flow (Fig. 9a), significantly lower values of $\langle p_z \rangle$

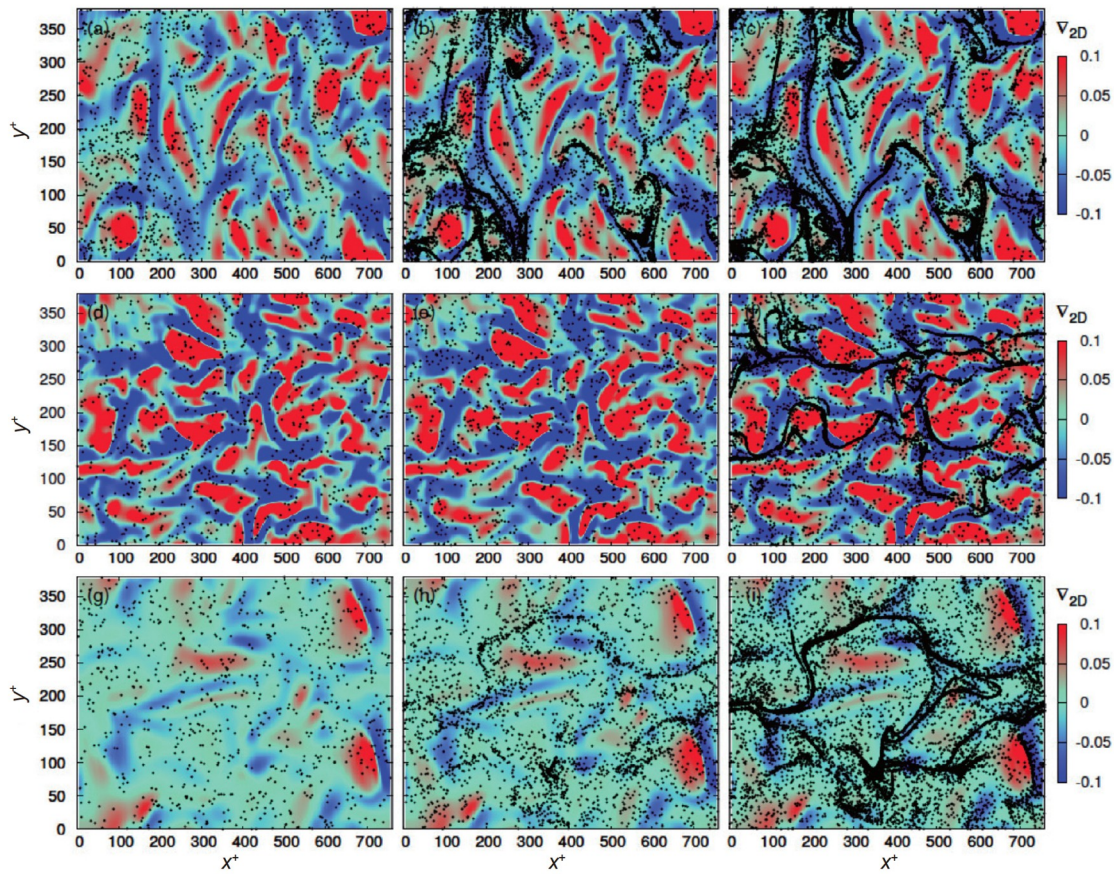

Figure 8 Instantaneous spatial distribution of gyrotactic micro-swimmers on the free surface of a turbulent Poiseuille flow in an open channel at $Re_\tau = 170$ without wind (top-row panels), with co-current wind (middle-row panels), and with counter-current wind (bottom-row panels). Panels in the left-hand column refer to swimmers with low gyrotaxis ($\Psi_L = 0.0113$); panels in the central column refer to swimmers with intermediate gyrotaxis ($\Psi_I = 0.113$); panels in the right-hand column refer to swimmers with high gyrotaxis ($\Psi_H = 1.13$). Figure taken from Ref. [13].

are observed within the wind-induced high-shear surface layer both with co-current wind (Fig. 9b) and counter-current wind (Fig. 9c). This mean-shear effect becomes more evident when $\Psi_K^+ \cong 1$.

It was observed that, once swimmers trespass the high-shear region and reach the surface, they tend to align in the horizontal flow direction because wall-normal turbulent fluctuations decay to zero and swimmers are brought about only by the residual fluid velocities in the horizontal direction [3,13]. Overall, wind is found to have a significant damping effect on the surfacing of the swimmers, which exhibit a narrower vertical spreading within the flow. Only organisms with high-enough gyrotaxis can maintain their ability to swim upwards.

Interestingly, a similar behaviour of the mean orientation was observed in the presence of temperature-induced stable stratification [11], which appears to hinder surfacing and damp vertical mixing when temperature gradients are large enough to generate thermoclines and internal gravity waves. Thermal stratification in water bodies influences the heat, momentum and chemical species exchange across the air-water interface by modifying the sub-surface turbulence characteristics. This is associated with the formation of internal gravity waves [58,61,62] near the free surface and above regions of well-mixed turbulence and active bursting phenomena. These waves correlate well with the so-called thermoclines, namely regions of the flow characterised by strong temperature gradients and poor mixing [55,63], which act as thermal barrier for organic and inorganic matter.

The modifications induced by stratification may affect the capability of the swimmers to reach the heated surface. An example is provided in Fig. 10, where the time evolution of the normalized swimmer concentration, C/C_0, along the vertical direction is shown. This figure shows that the rising of the swimmers depends strongly on the strength of stratification (quantified here by the shear Richardson number, Ri), especially near the thermocline where hydrodynamic shear may disrupt directional swimming and hinder near-surface accumulation. Indeed, a reduction of the cell rising speed and a temporary confinement under the thermocline was observed for all gyrotactic re-orientation times con-

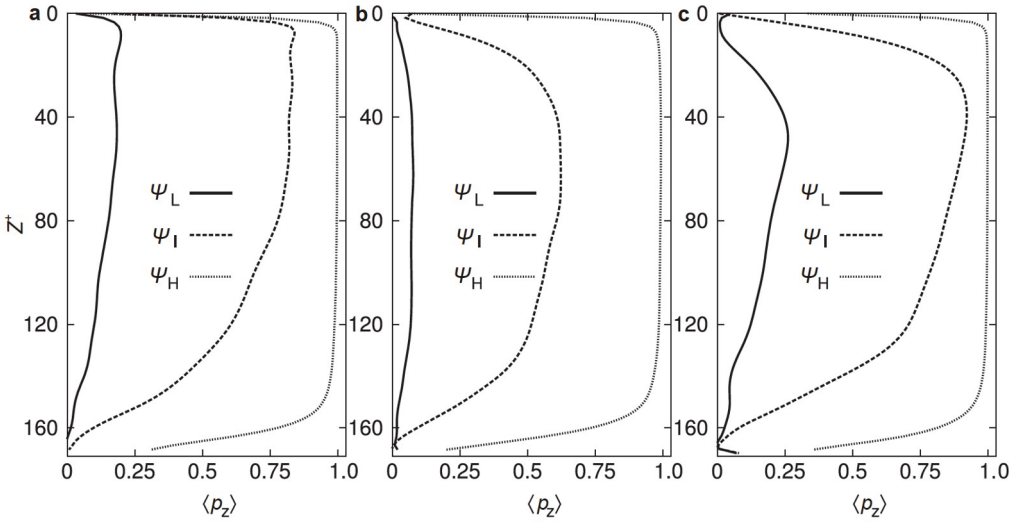

Figure 9 Mean orientation of the swimmers along the wall-normal direction, p_z at varying gyrotaxis (low gyrotaxis, $\Psi_L = 0.0113$: solid line; $\Psi_I = 0.113$: dashed line; high gyrotaxis, $\Psi_H = 1.13$: dotted line). The free surface is located at $Z^+ = 0$. **a** Free-slip surface; **b** co-current wind; **c** counter-current wind. Figure taken from [13].

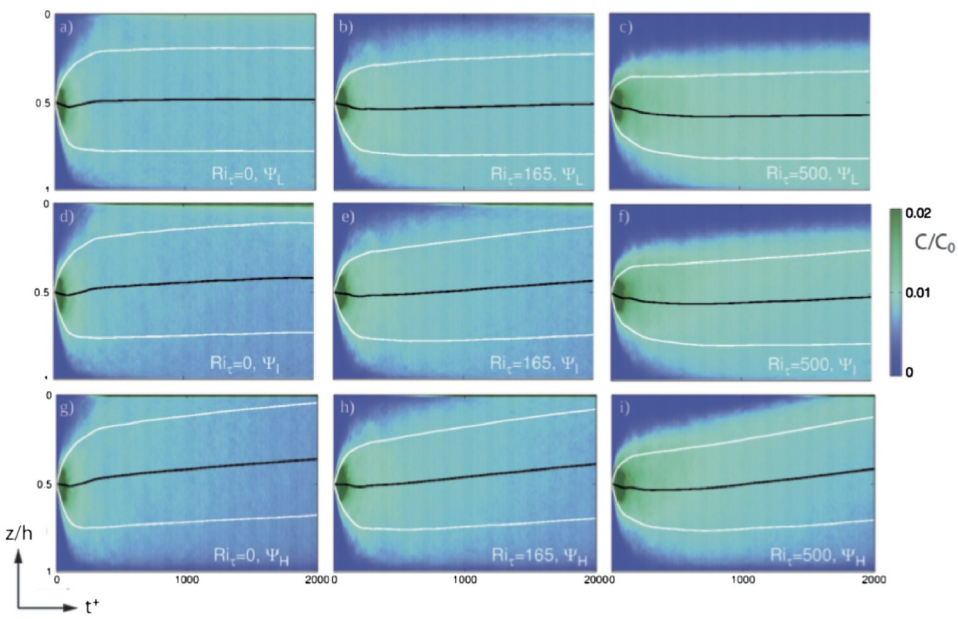

Figure 10 Time evolution of the swimmer concentration across the channel height, C/C_0, with $C = C(z, t)$ and $C_0 = C(z, t = 0)$. Top row: swimmers with low gyrotaxis, Ψ_L; middle row: swimmers with intermediate gyrotaxis, Ψ_I; bottom row: swimmers with high gyrotaxis, Ψ_H. Left-hand column: low stratification, $Ri_\tau = 0$; middle column: intermediate stratification, $Ri_\tau = 165$; right-hand column: high stratification, $Ri_\tau = 500$. The black line in each panel represents the center of mass of the swimmer distribution, and the white lines represent the standard deviation above and below the center of mass. Figure taken from Ref. [11].

sidered in Ref. [11] and swimmers eventually trespass the thermocline only if their re-orientation time is sufficiently small to ensure that the favourable condition for surfacing, $\Psi_K^+ > 1$, is met. If re-orientation is too slow (namely if $\Psi_K^+ < 1$), then the confinement lasts longer because vertical swimming is hampered and swimmers are forced to align in the horizontal direction.

These findings refer to inertialess swimmers, and so preferential orientation and clustering depend only on the interplay between gyrotaxis and turbulence. In the case of inertial organisms, we are only aware of the work by Sozza et al. [64], who however considered non-motile floaters transported by stratified turbulence. In spite of the different motility properties, it is interesting to observe that also floaters tend to accumulate within a thin layer around the fluid isopycnal produced by stratification, as a result of the

competing action of buoyancy (which attracts the floater to the isopycnal) and inertia (which prevents the floater from following the isopycnal exactly).

More recently, Ouillon et al. [65] have explored the collective vertical migration of a swarm of inertial swimmers through a stably stratified density interface, showing that the hydrodynamic interaction among the swimmers can produce a spatially coherent source of thrust that results in the formation of a swarm-scale jet in the direction opposite to the migration. Hydrodynamic interaction was not accounted for in Ref. [11] and may provide a further mean to optimize vertical migration.

The effects just described (turbulent advection, wind, stratification) may have important consequences for environmental processes such as spring phytoplankton bloom and growth, which are known to occur when turbulent mixing is sufficiently weak. For instance, Tergolina et al. [66] have explored the role of large-scale advection and small-scale turbulent diffusion in a kinematic flow field that accounts for well-controlled different spatial and temporal scales of the turbulent motions. Their results indicate that the large-scale coherent structures have an overwhelming importance on vertical phytoplankton dynamics of phytoplankton life cycles, which are only weakly affected by smaller-scale motions in realistic oceanic flow conditions.

6. Summary and future perspectives

In this review, we have summarized recent numerical results that show how substantial is the contribution of directional swimming to the dynamics of phytoplankton evolving in a turbulent flow, even when turbulence is significant. The main macroscopic effect associated to directional swimming is the occurrence of preferential concentration phenomena, which gives raise to swimmer segregation into densely-populated patches or clusters (depending on the specific properties of the turbulent flow field). Results from numerical simulations show that the degree of segregation can be "tuned" by modulating the vertical stability of directional swimming. These findings are in agreement with experimental observations [4] that some phytoplankton species have developed an adaptive behavioural mechanism to retain swimming efficiency in turbulent flows.

We have also examined the effect of gyrotaxis on the orientational dynamics of the swimmers, showing how the dynamics depend on the relative magnitude between time scale of the change in orientation and the time scale of turbulence, e.g., characterizing the velocity gradients experienced along the trajectory of a swimmer. Clearly, the correlation between the time scale of gyrotaxis and the time scale of turbulence is also crucial to determine the efficiency with which the swimmers migrate vertically across the water layer. We have reported the results that demonstrate this in a relatively simple instance of turbulent flow (homogeneous and isotropic) but also in more complex and realistic flow features, such as stratification or wind-induced shear at the air-water interface.

In spite of the knowledge acquired by means of accurate numerical simulations, we believe there are many directions that still need to be explored or fully understood. For instance, micro-swimmers are known to exhibit an intriguing, highly-dynamic collective motion characterized by large-scale swirling and streaming patterns, usually referred to as active or biologically-generated turbulence [67,68], which is reminiscent of classical high-Reynolds-number hydrodynamic turbulence and has been proposed as an important contributor to nutrient transport and ocean mixing. There is evidence that aggregations of marine organisms with size of order $O(10^{-2}$ m) can produce turbulent dissipation rates of $O(10^{-5}$ W kg$^{-1})$ and Reynolds numbers of $O(10^5)$, which would be comparable to strong wind and buoyancy forcing near the air-water interface [69]. In a recent study [68], squirmers embedded in a mesoscale fluid have been considered to explore the collective behaviour of bacteria-type micro-swimmers via coarse-grained mesoscale hydrodynamic simulations, showing the formation of clusters, activity-induced phase separation, and swarming behaviour. These findings emphasize the importance of the hydrodynamic flow field for swarming motility and bacterial turbulence [68], and confirm previous observations that purely hydrodynamic effects can alter the ecology of microorganisms that can vary their shape and their preferential orientation [4].

Another direction of interest is to investigate the effect of convective fluid inertia. Recent studies showed that spheroidal particles are subjected to a convective fluid inertial torque whenever they settle [70,71]. If the particle acquires motility and moves in the direction of its symmetry axis, this inertial torque drives the particle to swim upwards, acting as an effective gyrotaxis mechanism [29]. However, how this mechanism is modified by the propulsion mechanism of the swimmer still needs further investigation. On the other hand, while the inertial effect of unsteady fluid accelerations on motile organisms and the inertial forces that such organisms experience in steady shear flow can be directly inferred from the corresponding results for passive particles, the correct inclusion of convective inertial corrections to the history force on an active swimmer remains an open problem, since it is unclear how to extend the corrections known for passive particles [30].

Finally, current state of the art has not yet disentangled the effects associated to the biological processes that can affect population dynamics. Clearly, in situations where the characteristic time of directional swimming becomes the order of the characteristic time of population growth, the interplay

between purely biological (population growth) and physico-biological mechanisms (buoyancy control) becomes crucial [15]. This interplay should be addressed in future studies. In addition, current models still fail to reproduce faithfully the response of the swimmers to mechanical stresses [15], in order to quantify correctly the physiological responses to hydrodynamic stresses. However, this will require measurements of the changes in the vertical migration rate when cells are exposed to realistic turbulent flow conditions, representative of oceanic turbulence.

Author contributions *Jingran Qiu and Lihao Zhao investigated the current progress on the relevant studies and wrote sections 2, 3, 4 of the paper. Cristian Marchioli investigated the current progress on the relevant studies and wrote sections 1, 5, 6 of the paper. All authors participated in edit and review of the paper.*

Acknowledgements *This work was supported by the National Natural Science Foundation of China (Grant Nos. 11911530141 and 91752205).*

1 M. A. Bees, Advances in bioconvection, Annu. Rev. Fluid Mech. **52**, 449 (2020).
2 J. S. Guasto, R. Rusconi, and R. Stocker, Fluid mechanics of planktonic microorganisms, Annu. Rev. Fluid Mech. **44**, 373 (2012).
3 S. Lovecchio, C. Marchioli, and A. Soldati, Time persistence of floating-particle clusters in free-surface turbulence, Phys. Rev. E **88**, 33003 (2013).
4 A. Sengupta, F. Carrara, and R. Stocker, Phytoplankton can actively diversify their migration strategy in response to turbulent cues, Nature **543**, 555 (2017).
5 T. J. Pedley, and J. O. Kessler, Hydrodynamic phenomena in suspensions of swimming microorganisms, Annu. Rev. Fluid Mech. **24**, 313 (1992).
6 T. J. Pedley, and J. O. Kessler, A new continuum model for suspensions of gyrotactic micro-organisms, J. Fluid Mech. **212**, 155 (1990).
7 M. M. Dekshenieks, P. L. Donaghay, J. M. Sullivan, J. Rines, T. R. Osborn, and M. S. Twardowski, Temporal and spatial occurrence of thin phytoplankton layers in relation to physical processes, Mar. Ecol. Prog. Ser. **223**, 61 (2001).
8 W. M. Durham, E. Climent, M. Barry, F. De Lillo, G. Boffetta, M. Cencini, and R. Stocker, Turbulence drives microscale patches of motile phytoplankton, Nat. Commun. **4**, 2148 (2013).
9 F. De Lillo, M. Cencini, W. M. Durham, M. Barry, R. Stocker, E. Climent, and G. Boffetta, Turbulent fluid acceleration generates clusters of gyrotactic microorganisms, Phys. Rev. Lett. **112**, 44502 (2014).
10 K. Gustavsson, F. Berglund, P. R. Jonsson, and B. Mehlig, Preferential sampling and small-scale clustering of gyrotactic microswimmers in turbulence, Phys. Rev. Lett. **116**, 108104 (2016).
11 S. Lovecchio, F. Zonta, C. Marchioli, and A. Soldati, Thermal stratification hinders gyrotactic micro-organism rising in free-surface turbulence, Phys. Fluids **29**, 053302 (2017).
12 C. Marchioli, H. Bhatia, G. Sardina, L. Brandt, and A. Soldati, Role of large-scale advection and small-scale turbulence on vertical migration of gyrotactic swimmers, Phys. Rev. Fluids **4**, 124304 (2019).
13 M. Mashayekhpour, C. Marchioli, S. Lovecchio, E. N. Lay, and A. Soldati, Wind effect on gyrotactic micro-organism surfacing in free-surface turbulence, Adv. Water Resour. **129**, 328 (2019).
14 C. Zhan, G. Sardina, E. Lushi, and L. Brandt, Accumulation of motile elongated micro-organisms in turbulence, J. Fluid Mech. **739**, 22 (2014).
15 M. Cencini, G. Boffetta, M. Borgnino, and F. De Lillo, Gyrotactic phytoplankton in laminar and turbulent flows: A dynamical systems approach, Eur. Phys. J. E **42**, 1 (2019).
16 X. Chen, Y. Wu, and L. Zeng, Migration of gyrotactic micro-organisms in water, Water **10**, 1455 (2018).
17 Z. Liu, L. Jiang, and C. Sun, Accumulation and alignment of elongated gyrotactic swimmers in turbulence, Phys. Fluids **34**, 033303 (2022).
18 J. O. Kessler, Hydrodynamic focusing of motile algal cells, Nature **313**, 218 (1985).
19 J. O. Kessler, Individual and collective fluid dynamics of swimming cells, J. Fluid Mech. **173**, 191 (1986).
20 J. O. Kessler, Co-operative and concentrative phenomena of swimming micro-organisms, Contemp. Phys. **26**, 147 (1985).
21 W. M. Durham, J. O. Kessler, and R. Stocker, Disruption of vertical motility by shear triggers formation of thin phytoplankton layers, Science **323**, 1067 (2009).
22 M. Borgnino, G. Boffetta, F. De Lillo, and M. Cencini, Gyrotactic swimmers in turbulence: Shape effects and role of the large-scale flow, J. Fluid Mech. **856**, R1 (2018).
23 J. L. O. Almerol, and M. P. Liponhay, Clustering of fast gyrotactic particles in low-Reynolds-number flow, PLoS One **17**, e0266611 (2022).
24 J. Qiu, C. Marchioli, H. I. Andersson, and L. Zhao, Settling tracer spheroids in vertical turbulent channel flows, Int. J. Multiphase Flow **118**, 173 (2019).
25 M. Niazi Ardekani, G. Sardina, L. Brandt, L. Karp-Boss, R. N. Bearon, and E. A. Variano, Sedimentation of inertia-less prolate spheroids in homogenous isotropic turbulence with application to non-motile phytoplankton, J. Fluid Mech. **831**, 655 (2017).
26 S. Kim, and S. J. Karrila, Microhydrodynamics: Principles and Selected Applications (Butterworth-Heinemann, Oxford, 2013).
27 T. J. Pedley, and J. O. Kessler, The orientation of spheroidal microorganisms swimming in a flow field, Proc. R. Soc. Lond. B. **231**, 47 (1987).
28 F. Candelier, J. Qiu, L. Zhao, G. Voth, and B. Mehlig, Inertial torque on a squirmer, arXiv: 2209.03129.
29 J. Qiu, Z. Cui, E. Climent, and L. Zhao, Gyrotactic mechanism induced by fluid inertial torque for settling elongated microswimmers, Phys. Rev. Res. **4**, 23094 (2022).
30 T. Redaelli, F. Candelier, R. Mehaddi, and B. Mehlig, Unsteady and inertial dynamics of a small active particle in a fluid, Phys. Rev. Fluids **7**, 44304 (2022).
31 T. J. Smayda, Adaptations and selection of harmful and other dinoflagellate species in upwelling systems. 2. Motility and migratory behaviour, Prog. Oceanography **85**, 71 (2010).
32 J. Titelman, and T. Kiørboe, Motility of copepod nauplii and implications for food encounter, Mar. Ecol. Prog. Ser. **247**, 123 (2003).
33 D. Kamykowski, R. E. Reed, and G. J. Kirkpatrick, Comparison of sinking velocity, swimming velocity, rotation and path characteristics among six marine dinoflagellate species, Mar. Biol. **113**, 319 (1992).
34 S. O'Malley, and M. A. Bees, The orientation of swimming biflagellates in shear flows, Bull. Math. Biol. **74**, 232 (2012).
35 M. H. Sohn, K. W. Seo, Y. S. Choi, S. J. Lee, Y. S. Kang, and Y. S. Kang, Determination of the swimming trajectory and speed of chain-forming dinoflagellate Cochlodinium polykrikoides with digital holographic particle tracking velocimetry, Mar. Biol. **158**, 561 (2011).
36 G. J. Thorn, and R. N. Bearon, Transport of spherical gyrotactic organisms in general three-dimensional flow fields, Phys. Fluids **22**, 041902 (2010).
37 I. Fouxon, and A. Leshansky, Phytoplankton's motion in turbulent ocean, Phys. Rev. E **92**, 13017 (2015).
38 D. M. Lewis, The orientation of gyrotactic spheroidal micro-organisms in a homogeneous isotropic turbulent flow, Proc. R. Soc. Lond. A **459**, 1293 (2003).
39 E. J. Hinch, and L. G. Leal, The effect of Brownian motion on the rheological properties of a suspension of non-spherical particles, J.

Fluid Mech. **52**, 683 (1972).
40 H. Brenner, Rheology of a dilute suspension of axisymmetric Brownian particles, Int. J. Multiphase Flow **1**, 195 (1974).
41 R. Ni, N. T. Ouellette, and G. A. Voth, Alignment of vorticity and rods with Lagrangian fluid stretching in turbulence, J. Fluid Mech. **743**, R3 (2014).
42 L. Zhao, and H. I. Andersson, Why spheroids orient preferentially in near-wall turbulence, J. Fluid Mech. **807**, 221 (2016).
43 M. Borgnino, K. Gustavsson, F. De Lillo, G. Boffetta, M. Cencini, and B. Mehlig, Alignment of nonspherical active particles in chaotic flows, Phys. Rev. Lett. **123**, 138003 (2019).
44 P. Tiselius, P. R. Jonsson, and P. G. Verity, A model evaluation of the impact of food patchiness on foraging strategy and predation risk in zooplankton, Bull. Mar. Sci. **53**, 247 (1993).
45 D. A. Siegel, Resource competition in a discrete environment: Why are plankton distributions paradoxical? Limnol. Oceanogr. **43**, 1133 (1998).
46 S. Lovecchio, E. Climent, R. Stocker, and W. M. Durham, Chain formation can enhance the vertical migration of phytoplankton through turbulence, Sci. Adv. **5**, 7879 (2019).
47 F. G. Michalec, S. Souissi, and M. Holzner, Turbulence triggers vigorous swimming but hinders motion strategy in planktonic copepods, J. R. Soc. Interface. **12**, 20150158 (2015).
48 R. Monchaux, M. Bourgoin, and A. Cartellier, Preferential concentration of heavy particles: A Voronoï analysis, Phys. Fluids **22**, 103304 (2010).
49 Y. Tagawa, J. M. Mercado, V. N. Prakash, E. Calzavarini, C. Sun, and D. Lohse, Three-dimensional Lagrangian Voronoï analysis for clustering of particles and bubbles in turbulence, J. Fluid Mech. **693**, 201 (2012).
50 U. Frisch, and A. N. Kolmogorov, Turbulence: The Legacy of A. N. Kolmogorov (Cambridge University Press, Cambridge, 1995).
51 G. Falkovich, K. Gawędzki, and M. Vergassola, Particles and fields in fluid turbulence, Rev. Mod. Phys. **73**, 913 (2001).
52 I. Fouxon, Distribution of particles and bubbles in turbulence at a small Stokes number, Phys. Rev. Lett. **108**, 134502 (2012).
53 W. M. Durham, E. Climent, and R. Stocker, Gyrotaxis in a steady vortical flow, Phys. Rev. Lett. **106**, 238102 (2011).
54 S. Lovecchio, F. Zonta, and A. Soldati, Influence of thermal stratification on the surfacing and clustering of floaters in free surface turbulence, Adv. Water Resour. **72**, 22 (2014).
55 A. Jaccod, S. Berti, E. Calzavarini, and S. Chibbaro, Predator-prey plankton dynamics in turbulent flow past an obstacle, Phys. Rev. Fluids **6**, 103802 (2021).
56 J. Qiu, N. Mousavi, K. Gustavsson, C. Xu, B. Mehlig, and L. Zhao, Navigation of micro-swimmers in steady flow: The importance of symmetries, J. Fluid Mech. **932**, A10 (2022).
57 R. M. Enriquez, and J. R. Taylor, Numerical simulations of the competition between wind-driven mixing and surface heating in triggering spring phytoplankton blooms, ICES J. Mar. Sci. **72**, 1926 (2015).
58 F. Zonta, M. Onorato, and A. Soldati, Turbulence and internal waves in stably-stratified channel flow with temperature-dependent fluid properties, J. Fluid Mech. **697**, 175 (2012).
59 P. Gutiérrez, and S. Aumaître, Clustering of floaters on the free surface of a turbulent flow: An experimental study, Eur. J. Mech.-B Fluids **60**, 24 (2016).
60 S. Lovecchio, F. Zonta, and A. Soldati, Upscale energy transfer and flow topology in free-surface turbulence, Phys. Rev. E **91**, 33010 (2015).
61 R. Ferrari, and C. Wunsch, Ocean circulation kinetic energy: Reservoirs, sources, and sinks, Annu. Rev. Fluid Mech. **41**, 253 (2009).
62 P. Hingsamer, F. Peeters, and H. Hofmann, The consequences of internal waves for phytoplankton focusing on the distribution and production of Planktothrix rubescens, PLoS One **9**, e104359 (2014).
63 W. D. Smyth, and J. N. Moum, Length scales of turbulence in stably stratified mixing layers, Phys. Fluids **12**, 1327 (2000).
64 A. Sozza, F. De Lillo, and G. Boffetta, Inertial floaters in stratified turbulence, Europhys. Lett. **121**, 14002 (2018).
65 R. Ouillon, I. A. Houghton, J. O. Dabiri, and E. Meiburg, Active swimmers interacting with stratified fluids during collective vertical migration, J. Fluid Mech. **902**, A23 (2020).
66 V. B. Tergolina, E. Calzavarini, G. Mompean, and S. Berti, Effects of large-scale advection and small-scale turbulent diffusion on vertical phytoplankton dynamics, Phys. Rev. E **104**, 65106 (2021).
67 I. A. Houghton, J. R. Koseff, S. G. Monismith, and J. O. Dabiri, Vertically migrating swimmers generate aggregation-scale eddies in a stratified column, Nature **556**, 497 (2018).
68 K. Qi, E. Westphal, G. Gompper, and R. G. Winkler, Emergence of active turbulence in microswimmer suspensions due to active hydrodynamic stress and volume exclusion, Commun. Phys. **5**, 49 (2022).
69 E. Kunze, Biologically generated mixing in the ocean, Annu. Rev. Mar. Sci. **11**, 215 (2019).
70 K. Gustavsson, M. Z. Sheikh, D. Lopez, A. Naso, A. Pumir, and B. Mehlig, Effect of fluid inertia on the orientation of a small prolate spheroid settling in turbulence, New J. Phys. **21**, 083008 (2019).
71 F. Jiang, L. Zhao, H. I. Andersson, K. Gustavsson, A. Pumir, and B. Mehlig, Inertial torque on a small spheroid in a stationary uniform flow, Phys. Rev. Fluids **6**, 24302 (2021).

湍流中的趋旋性主动粒子研究进展

邱敬然, Cristian Marchioli, 赵立豪

摘要 许多海洋浮游生物能够主动运动. 它们会在昼夜间进行垂向的迁徙, 穿过数十米高的水层. 微小的浮游生物是如何在湍流环境中实现定向迁移的呢? 趋旋稳定性是其中一种机制, 其表现为浮游生物在重力作用下倾向于沿着特定方向游动. 由于特定机制, 如细胞的质量非均匀分布, 许多浮游生物受到一种由重力引起的力矩, 使其面朝重力的反方向游动. 然而, 其游动方向往往会被海洋湍流中的剪切和速度脉动扰乱: 这些扰动产生的黏性力矩会让浮游生物的游动方向失稳. 在重力力矩和黏性力矩的共同作用下, 浮游生物朝特定方向的运动特性便被称为趋旋性. 人们发现这一机制能够导致浮游生物的非均匀分布, 使它们形成团簇或者薄层. 这些现象由流体运动引起的非线性动力学过程决定, 而这一领域的研究正吸引越来越多的关注. 将Navier-Stokes方程的与趋旋游动粒子的模型方程结合的数值模拟方法受到广泛使用, 并展现出其潜力. 该方法能够让人们能够深入研究自推进粒子的动力学和统计学性质. 在本文中, 我们对湍流中趋旋粒子的近期关键进展进行了综述. 首先, 我们介绍了关于趋旋粒子的朝向和它们垂向迁移的相关研究. 其次, 我们讨论了关于趋旋粒子聚集性的研究. 最后, 我们回顾了壁湍流中的趋旋粒子运动行为的相关研究.